

# The challenge for single field inflation with BICEP2 result

Qing Gao<sup>1,\*</sup> and Yungui Gong<sup>1,2,†</sup>

<sup>1</sup>MOE Key Laboratory of Fundamental Quantities Measurement, School of Physics,  
Huazhong University of Science and Technology, Wuhan 430074, P. R. China

<sup>2</sup>Institute of Theoretical Physics, Chinese Academy of Sciences, Beijing 100190, P. R. China

The detection of B-mode power spectrum by the BICEP2 collaboration constrains the tensor-to-scalar ratio  $r = 0.20_{-0.05}^{+0.07}$  for the lensed- $\Lambda$ CDM model. The consistency of this big value with the *Planck* results requires a large running of the spectral index. The large values of the tensor-to-scalar ratio and the running of the spectral index put a challenge to single field inflation. For the chaotic inflation, the larger the value of the tensor-to-scalar ratio is, the smaller the value of the running of the spectral index is. For the natural inflation, the absolute value of the running of the spectral index has an upper limit.

PACS numbers: 98.80.Cq, 98.80.Es

## I. INTRODUCTION

The detection of the primordial B-mode power spectrum by the BICEP2 collaboration confirms the existence of primordial gravitational wave, and the observed B-mode power spectrum gives the constraint on the tensor-to-scalar ratio with  $r = 0.20_{-0.05}^{+0.07}$  at  $1\sigma$  level for the lensed- $\Lambda$ CDM model [1]. Furthermore,  $r = 0$  is disfavored at  $7.0\sigma$  level. The new constraints on  $r$  and the spectral index  $n_s$  exclude a wide class of inflationary models. For the inflation model with non-minimal coupling with gravity [2], a universal attractor at strong coupling was found with  $n_s = 1 - 2/N$  and  $r = 12/N^2$ . This model is inconsistent with the BICEP2 result  $r \gtrsim 0.1$  at  $2\sigma$  level because the BICEP2 constraint on  $r$  requires the number of e-folds  $N = \sqrt{12/r} \lesssim \sqrt{120} \approx 11$  which is not enough to solve the horizon problem. If we require  $N = 50$ , then  $r = 0.0048$ , so the model is excluded by the BICEP2 result. For the small-field inflation like the hilltop inflation with the potential  $V(\phi) = V_0[1 - (\phi/\mu)^p]$  [3, 4],  $r \sim 0$ , so the model is excluded by the BICEP2 result.

Without the running of the spectral index, the combination of *Planck*+WP+highL data gives  $n_s = 0.9600 \pm 0.0072$  and  $r_{0.002} < 0.0457$  at the 68% confidence level for the  $\Lambda$ CDM model [5, 6] which is in tension with the BICEP2 result. When the running of the spectral index is included in the data fitting, the same combination gives  $n_s = 0.957 \pm 0.015$ ,  $n'_s = dn_s/d \ln k = -0.022_{-0.021}^{+0.020}$  and  $r_{0.002} < 0.263$  at the 95% confidence level [5, 6]. To give a consistent constraint on  $r$  for the combination of *Planck*+WP+highL data and the BICEP2 data, we require a running of the spectral index  $n'_s < -0.002$  at the 95% confidence level. For the single field inflation, the spectral index  $n_s$  for the scalar perturbation deviates from the Harrison-Zel'dovich value of 1 in the order of  $10^{-2}$ , so  $n'_s$  is in the order of  $10^{-3}$ . The explanation of

large  $r$  and  $n'_s$  is a challenge to single field inflation. In light of the BICEP2 data, several attempts were proposed to explain the large value of  $r$  [7–30]. In this Letter, we use the chaotic and natural inflation models to explain the challenge.

## II. SLOW-ROLL INFLATION

The slow-roll parameters are defined as

$$\epsilon = \frac{M_{pl}^2 V_\phi^2}{2V^2}, \quad (1)$$

$$\eta = \frac{M_{pl}^2 V_{\phi\phi}}{V}, \quad (2)$$

$$\xi = \frac{M_{pl}^4 V_\phi V_{\phi\phi\phi}}{V^2}, \quad (3)$$

where  $M_{pl}^2 = (8\pi G)^{-1}$ ,  $V_\phi = dV(\phi)/d\phi$ ,  $V_{\phi\phi} = d^2V(\phi)/d\phi^2$  and  $V_{\phi\phi\phi} = d^3V(\phi)/d\phi^3$ . For the single field inflation, the spectral indices, the tensor-to-scalar ratio and the running are given by

$$n_s - 1 \approx 2\eta - 6\epsilon, \quad (4)$$

$$r \approx 16\epsilon \approx -8n_t, \quad (5)$$

$$n'_s = dn_s/d \ln k \approx 16\epsilon\eta - 24\epsilon^2 - 2\xi. \quad (6)$$

The number of e-folds before the end of inflation is given by

$$N(t) = \int_t^{t_e} H dt \approx \frac{1}{M_{pl}^2} \int_{\phi_e}^{\phi} \frac{V(\phi)}{V_\phi(\phi)} d\phi, \quad (7)$$

where the value  $\phi_e$  of the inflaton field at the end of inflation is defined by  $\epsilon(\phi_e) = 1$ . The scalar power spectrum is

$$\mathcal{P}_{\mathcal{R}} = A_s \left( \frac{k}{k_*} \right)^{n_s - 1 + n'_s \ln(k/k_*)/2}, \quad (8)$$

\* gaoqing01good@163.com

† yggong@mail.hust.edu.cn

where the subscript “\*” means the value at the horizon crossing, the scalar amplitude

$$A_s \approx \frac{1}{24\pi^2 M_{pl}^4} \frac{\Lambda^4}{\epsilon}. \quad (9)$$

With the BICEP2 result  $r = 0.2$ , the energy scale of inflation is  $\Lambda \sim 2.2 \times 10^{16} \text{GeV}$ .

For the chaotic inflation with the power-law potential  $V(\phi) = \Lambda^4 (\phi/M_{pl})^p$  [31], the slow-roll parameters are  $\epsilon = p/(4N_*)$ ,  $\eta = (p-1)/(2N_*)$  and  $\xi = (p-1)(p-2)/(4N_*^2)$ . The spectral index  $n_s = 1 - (p+2)/(2N_*)$ , the running of the spectral index  $n'_s = -(2+p)/(2N_*^2) = -2(1-n_s)^2/(p+2) < 0$  and the tensor-to-scalar ratio  $r = 4p/N_* = 8p(1-n_s)/(p+2)$ . We plot the  $n_s - r$  and  $n_s - n'_s$  relations in Figs. 1 and 2 for  $p = 1, p = 2, p = 3$  and  $p = 4$ . In Fig. 1, we also show the points with  $N_* = 50$  and  $N_* = 60$ . From Figs. 1 and 2, we see that  $r$  increases with the power  $p$ , but  $|n'_s|$  decreases with the power  $p$ . Therefore, it is not easy to satisfy both the requirements  $r \gtrsim 0.1$  and  $n'_s < -0.002$ . The chaotic inflation with  $2 < p < 3$  is marginally consistent with the observation at the 95% confidence level.

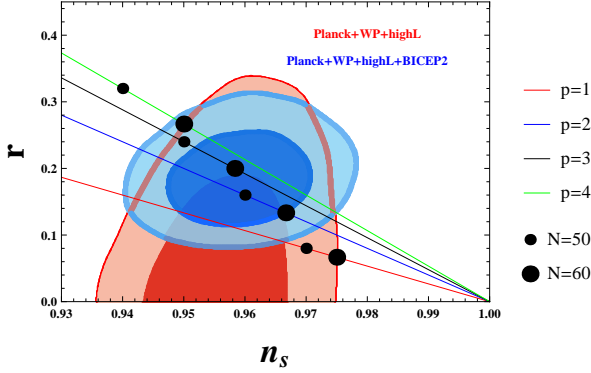


FIG. 1. The  $n_s - r$  diagrams for the chaotic inflation with  $p = 1, p = 2, p = 3$  and  $p = 4$ . The 68% and 95% confidence contours from the *Planck*+WP+highL data [5, 6] and the *Planck*+WP+highL+BICEP2 data [1] for the  $\Lambda$ CDM model are also shown.

For the natural inflation with the potential  $V(\phi) = \Lambda^4 [1 + \cos(\phi/f)]$  [32], the slow-roll parameters are

$$\epsilon = \frac{M_{pl}^2}{2f^2} \left[ \frac{\sin(\phi/f)}{1 + \cos(\phi/f)} \right]^2, \quad (10)$$

$$\eta = -\frac{M_{pl}^2}{f^2} \frac{\cos(\phi/f)}{1 + \cos(\phi/f)}, \quad (11)$$

$$\xi = -\frac{M_{pl}^4}{f^4} \left[ \frac{\sin(\phi/f)}{1 + \cos(\phi/f)} \right]^2 = -\frac{2M_{pl}^2}{f^2} \epsilon. \quad (12)$$

Inflation ends when  $\epsilon \sim 1$ , so

$$\frac{\phi_e}{f} = \arccos \left[ \frac{1 - 2(f/M_{pl})^2}{1 + 2(f/M_{pl})^2} \right], \quad (13)$$

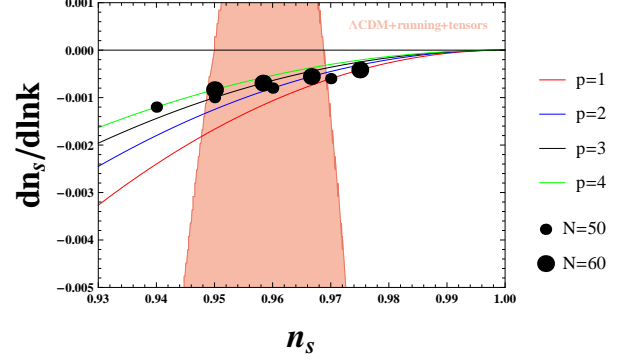


FIG. 2. The  $n_s - n'_s$  diagrams for the chaotic inflation with  $p = 1, p = 2, p = 3$  and  $p = 4$ . The 95% confidence contour for the  $\Lambda$ CDM model from the *Planck*+WP+highL data [5, 6] is also shown.

and the number of e-folds before the end of inflation is

$$N_* = \frac{2f^2}{M_{pl}^2} \ln \left[ \frac{\sin(\phi_e/2f)}{\sin(\phi_*/2f)} \right]. \quad (14)$$

Combining Eqs. (4)-(6) with (10)-(12), we plot the  $n_s - r$  and  $n_s - n'_s$  relations for the natural inflation with  $f = 5M_{pl}, f = 7M_{pl}, f = 10M_{pl}$  and  $f = 20M_{pl}$  in Figs. 3 and 4. In Fig. 3, we also show the points with  $N_* = 50$  and  $N_* = 60$ . The results show that both  $r$  and  $|n'_s|$  increase with the global symmetry breaking scale  $f$ . However, there is an upper limit on  $|n'_s|$  which is only marginally consistent with the observation at the 95% confidence level. When  $f/M_{mp} \gg 1$ , the potential can be approximated by  $V(\phi) = \Lambda^4 (\phi/f - \pi)^2/2$  which is the power-law potential with  $p = 2$ , this is the reason for the upper limit on  $n'_s$ .

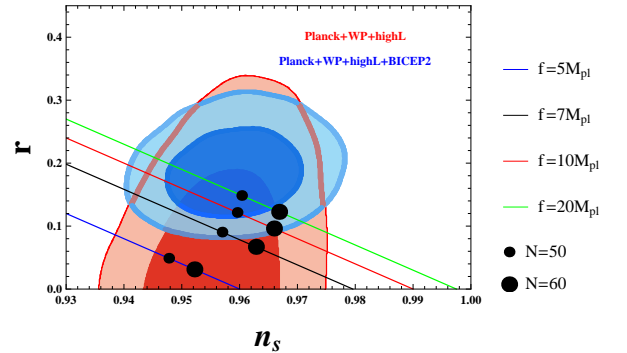


FIG. 3. The  $n_s - r$  diagrams for the natural inflation with  $f = 5M_{pl}, f = 7M_{pl}, f = 10M_{pl}$  and  $f = 20M_{pl}$ . The 68% and 95% confidence contours from the *Planck*+WP+highL data [5, 6] and the *Planck*+WP+highL+BICEP2 data [1] for the  $\Lambda$ CDM model are also shown.

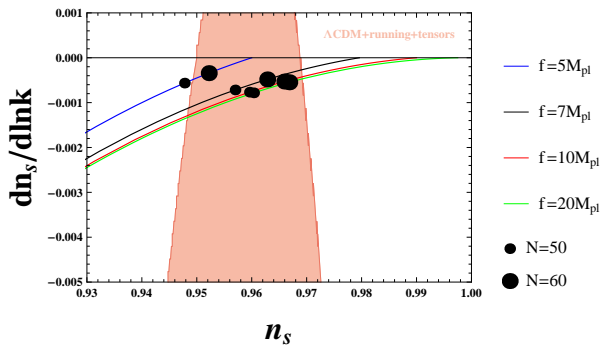


FIG. 4. The  $n_s - n'_s$  diagrams for the natural inflation with  $f = 5M_{pl}$ ,  $f = 7M_{pl}$ ,  $f = 10M_{pl}$  and  $f = 20M_{pl}$ . The 95% confidence contour for the  $\Lambda$ CDM model from the *Planck*+WP+highL data [5, 6] is also shown.

### III. CONCLUSIONS

For a single inflaton field with slow-roll, the tensor-to-scalar ratio  $r \approx 16\epsilon$  which is linear with the slow-roll parameter  $\epsilon$ , but the running of the spectral index  $n'_s$  depends on the second order slow-roll parameters, so  $n'_s$  is

at most in the order of  $10^{-3}$ . The BICEP2 and the *Planck* data constrain  $n'_s = -0.0221^{+0.011}_{-0.0099}$  and  $r = 0.20^{+0.07}_{-0.05}$  at the  $1\sigma$  confidence level. Both the chaotic and natural inflation are inconsistent with the observation at the  $1\sigma$  level. The chaotic inflation with  $2 < p < 3$  and the natural inflation with  $f \gtrsim 10M_{pl}$  are marginally consistent with the observation at the 95% confidence level. In conclusion, it is a challenge to simultaneously explain  $r$  as large as 0.2 and  $n'_s$  as large as  $-0.01$  for single field inflation. Unless the *Planck* and the BICEP2 data can be reconciled without large  $n'_s$ , the challenge to single field inflation remains.

### ACKNOWLEDGMENTS

This work was partially supported by the National Basic Science Program (Project 973) of China under grant No. 2010CB833004, the NNSF of China under grant No. 11175270, the Program for New Century Excellent Talents in University under grant No. NCET-12-0205 and the Fundamental Research Funds for the Central Universities under grant No. 2013YQ055.

- 
- [1] P. Ade *et al.*, BICEP2 I: Detection Of B-mode Polarization at Degree Angular Scales, [arXiv:1403.3985 \[astro-ph.CO\]](#), 2014.
  - [2] R. Kallosh, A. Linde, and D. Roest, *Phys. Rev. Lett.* 112 (2014) 011303.
  - [3] A. Albrecht and P.J. Steinhardt, *Phys. Rev. Lett.* 48 (1982) 1220.
  - [4] L. Boubekeur and D. Lyth, *J. Cosmol. Astropart. Phys.* 0507 (2005) 010.
  - [5] P. Ade *et al.*, Planck 2013 results. XVI. Cosmological parameters, [arXiv:1303.5076 \[astro-ph.CO\]](#), 2013.
  - [6] P. Ade *et al.*, Planck 2013 results. XXII. Constraints on inflation, [arXiv:1303.5082 \[astro-ph.CO\]](#), 2013.
  - [7] J. Lizarraga *et al.*, Can topological defects mimic the BICEP2 B-mode signal?, [arXiv:1403.4924 \[astro-ph.CO\]](#), 2014.
  - [8] K. Harigaya and T.T. Yanagida, Discovery of Large Scale Tensor Mode and Chaotic Inflation in Supergravity, [arXiv:1403.4729 \[hep-ph\]](#), 2014.
  - [9] C.R. Contaldi, M. Peloso, and L. Sorbo, Suppressing the impact of a high tensor-to-scalar ratio on the temperature anisotropies, [arXiv:1403.4596 \[astro-ph.CO\]](#), 2014.
  - [10] H. Collins, R. Holman, and T. Vardanyan, Do Mixed States save Effective Field Theory from BICEP?, [arXiv:1403.4592 \[hep-th\]](#), 2014.
  - [11] C.T. Byrnes, M. Cortés, and A.R. Liddle, Comprehensive analysis of the simplest curvaton model, [arXiv:1403.4591 \[astro-ph.CO\]](#), 2014.
  - [12] L.A. Anchordoqui, V. Barger, H. Goldberg, X. Huang, and D. Marfatia, S-dual inflation: BICEP2 data without unlikelihood, [arXiv:1403.4578 \[hep-ph\]](#), 2014.
  - [13] K. Harigaya, M. Ibe, K. Schmitz, and T.T. Yanagida, Dynamical Chaotic Inflation in the Light of BICEP2, [arXiv:1403.4536 \[hep-ph\]](#), 2014.
  - [14] K. Nakayama and F. Takahashi, Higgs Chaotic Inflation and the Primordial B-mode Polarization Discovered by BICEP2, [arXiv:1403.4132 \[hep-ph\]](#), 2014.
  - [15] W. Zhao, C. Cheng, and Q.-G. Huang, Hint of relic gravitational waves in the Planck and WMAP data, [arXiv:1403.3919 \[astro-ph.CO\]](#), 2014.
  - [16] J.L. Cook, L.M. Krauss, A.J. Long, and S. Sabharwal, Is Higgs Inflation Dead?, [arXiv:1403.4971 \[astro-ph.CO\]](#), 2014.
  - [17] T. Kobayashi and O. Seto, Polynomial inflation models after BICEP2, [arXiv:1403.5055 \[astro-ph.CO\]](#), 2014.
  - [18] V. Miranda, W. Hu, and P. Adshead, Steps to Reconcile Inflationary Tensor and Scalar Spectra, [arXiv:1403.5231 \[astro-ph.CO\]](#), 2014.
  - [19] I. Masina, The Gravitational Wave Background and Higgs False Vacuum Inflation, [arXiv:1403.5244 \[astro-ph.CO\]](#), 2014.
  - [20] Y. Hamada, H. Kawai, K.-y. Oda, and S.C. Park, Higgs inflation still alive, [arXiv:1403.5043 \[hep-ph\]](#), 2014.
  - [21] M.P. Hertzberg, Inflation, Symmetry, and B-Modes, [arXiv:1403.5253 \[hep-th\]](#), 2014.
  - [22] J.B. Dent, L.M. Krauss, and H. Mathur, Killing the Straw Man: Does BICEP Prove Inflation?, [arXiv:1403.5166 \[astro-ph.CO\]](#), 2014.
  - [23] J. Joergensen, F. Sannino, and O. Svendsen, BICEP2 hints towards Quantum Corrections for Non-Minimally Coupled Inflationary Theories, [arXiv:1403.3289 \[hep-ph\]](#), 2014.
  - [24] K. Freese and W.H. Kinney, Natural Inflation: Consistency with Cosmic Microwave Background Observations of Planck and BICEP2, [arXiv:1403.5277 \[astro-ph.CO\]](#), 2014.

- [25] A. Ashoorioon, K. Dimopoulos, M. Sheikh-Jabbari, and G. Shiu, Non-Bunch-Davis Initial State Reconciles Chaotic Models with BICEP and Planck, [arXiv:1403.6099 \[hep-th\]](#), 2014.
- [26] A. Ashoorioon, K. Dimopoulos, M. Sheikh-Jabbari, and G. Shiu, *J. Cosmol. Astropart. Phys.* 1402 (2014) 025.
- [27] S. Choudhury and A. Mazumdar, Reconstructing inflationary potential from BICEP2 and running of tensor modes, [arXiv:1403.5549 \[hep-th\]](#), 2014.
- [28] S. Choudhury and A. Mazumdar, *Nucl. Phys. B* 882 (2014) 386.
- [29] S. Hotchkiss, A. Mazumdar, and S. Nadathur, *J. Cosmol. Astropart. Phys.* 1202 (2012) 008.
- [30] I. Ben-Dayan and R. Brustein, *J. Cosmol. Astropart. Phys.* 1009 (2010) 007.
- [31] A.D. Linde, *Phys. Lett. B* 129 (1983) 177.
- [32] K. Freese, J.A. Frieman, and A.V. Olinto, *Phys. Rev. Lett.* 65 (1990) 3233.